

## Global Description of EUSO-Balloon Instrument

C. MORETTO<sup>1</sup>, S. DAGORET-CAMPAGNE<sup>1</sup>, J.H. ADAMS<sup>19</sup>, P. VON BALLMOOS<sup>2</sup>, P. BARRILLON<sup>1</sup>, J. BAYER<sup>5</sup>, M. BERTAINA<sup>12</sup>, S. BLIN-BONDIL<sup>1</sup>, F. CAFAGNA<sup>7</sup>, M. CASOLINO<sup>13,10,11</sup>, C. CATALANO<sup>2</sup>, P. DANTO<sup>4</sup>, A. EBERSOLDT<sup>6</sup>, T. EBISUZAKI<sup>13</sup>, J. EVRARD<sup>4</sup>, PH. GORODETZKY<sup>3</sup>, A. HAUNGS<sup>6</sup>, A. JUNG<sup>14</sup>, Y. KAWASAKI<sup>13</sup>, H. LIM<sup>14</sup>, G. MEDINA-TANCO<sup>15</sup>, H. MIYAMOTO<sup>1</sup>, D. MONNIER-RAGAIGNE<sup>1</sup>, T. OMORI<sup>13</sup>, G. OSTERIA<sup>9</sup>, E. PARIZOT<sup>3</sup>, I.H. PARK<sup>14</sup>, P. PICOZZA<sup>13,10,11</sup>, G. PRÉVÔT<sup>3</sup>, H. PRIETO<sup>13,17</sup>, M. RICCI<sup>8</sup>, M.D. RODRÍGUEZ FRÍAS<sup>17</sup>, A. SANTANGELO<sup>5</sup>, J. SZABELSKI<sup>16</sup>, Y. TAKIZAWA<sup>13</sup>, K. TSUNO<sup>13</sup> FOR THE JEM-EUSO COLLABORATION<sup>19</sup>.

<sup>1</sup> *Laboratoire de l'Accélérateur Linéaire, Université Paris Sud-11, CNRS/IN2P3, Orsay, France*

<sup>2</sup> *Institut de Recherche en Astrophysique et Planétologie, Toulouse, France*

<sup>3</sup> *AstroParticule et Cosmologie, Univ Paris Diderot, CNRS/IN2P3, Paris, France*

<sup>4</sup> *Centre National d'Études Spatiales, Centre Spatial de Toulouse, France*

<sup>5</sup> *Institute for Astronomy and Astrophysics, Kepler Center, University of Tübingen, Germany*

<sup>6</sup> *Karlsruhe Institute of Technology (KIT), Germany*

<sup>7</sup> *Istituto Nazionale di Fisica Nucleare - Sezione di Bari, Italy*

<sup>8</sup> *Istituto Nazionale di Fisica Nucleare - Laboratori Nazionali di Frascati, Italy*

<sup>9</sup> *Istituto Nazionale di Fisica Nucleare - Sezione di Napoli, Italy*

<sup>10</sup> *Istituto Nazionale di Fisica Nucleare - Sezione di Roma Tor Vergata, Italy*

<sup>11</sup> *Università di Roma Tor Vergata - Dipartimento di Fisica, Roma, Italy*

<sup>12</sup> *Dipartimento di Fisica dell'Università di Torino and INFN Torino, Torino, Italy*

<sup>13</sup> *RIKEN Advanced Science Institute, Wako, Japan*

<sup>14</sup> *Sungkyunkwan University, Suwon-si, Kyung-gi-do, Republic of Korea*

<sup>15</sup> *Universidad Nacional Autónoma de México (UNAM), Mexico*

<sup>16</sup> *National Centre for Nuclear Research, Lodz, Poland*

<sup>17</sup> *Universidad de Alcalá (UAH), Madrid, Spain*

<sup>18</sup> *University of Alabama in Huntsville, Huntsville, USA*

<sup>19</sup> <http://jemeuso.riken.jp>

*moretto@lal.in2p3.fr*

**Abstract:** The EUSO-Balloon is a pathfinder of the JEM-EUSO mission, designed to be installed on-board the International Space Station before the end of this decade. The EUSO-Balloon instrument, conceived as a scaled-down version of the main mission, is currently developed as a payload of a stratospheric balloon operated by CNES, and will, most likely, be launched during the CNES flight campaign in 2014. Several key elements of JEM-EUSO have been implemented in the EUSO-Balloon. The instrument consists of an UV telescope, made of three Fresnel lenses, designed to focus the signal of the UV tracks, generated by highly energetic cosmic rays propagating in the earth's atmosphere, onto a finely pixelized UV camera. In this contribution, we review the main stages of the signal processing of the EUSO-Balloon instrument: the photodetection, the analog electronics, the trigger stages, which select events while rejecting random background, the acquisition system performing data storage and the monitoring, which allows the instrument control during operation.

**Keywords:** JEM-EUSO, UHECR, space instrument, balloon experiment, instrumentation

## 1 Introduction

The EUSO-Balloon is an experiment aiming at validating the conceptual design as well as the technologies foreseen for the ultra high energy cosmic ray space-based observatory JEM-EUSO [1]. The instrument, a scaled-down version of JEM-EUSO, includes several of the key components of the main space mission. Scientific and technical goals of the balloon instrument are reviewed in [2] and its simulation is presented in [3]. The EUSO-Balloon instrument, designed as payload of a stratospheric balloon operated by CNES, will perform a series of night-flights, lasting from a few hours to tens of hours, at altitudes of  $\sim 40$  km, and at different locations. The proposed program requires payload recovery after landing either in water or ground, and the repairing of the instrument after each mission. Special atmospheric environmental conditions and recovery require-

ments imply a very careful design and dedicated tests on advanced prototypes.

The paper is organised as follows. First, section 2 gives an overview of the instrument, including its particular mechanical design adapted to balloon flights. Section 3 provides details on the subsystems and highlights the main reasons for the chosen design. Section 4 deals with all series of preliminary measurements and tests, mandatory before the acceptance of the instrument for the actual flight. Finally, control and analysis tasks to be performed during the operation, are mentioned in section 5.

## 2 The Instrument Overview

The EUSO-Balloon instrument structure is shown in figure 1 and its main characteristics are given in table 1. The main

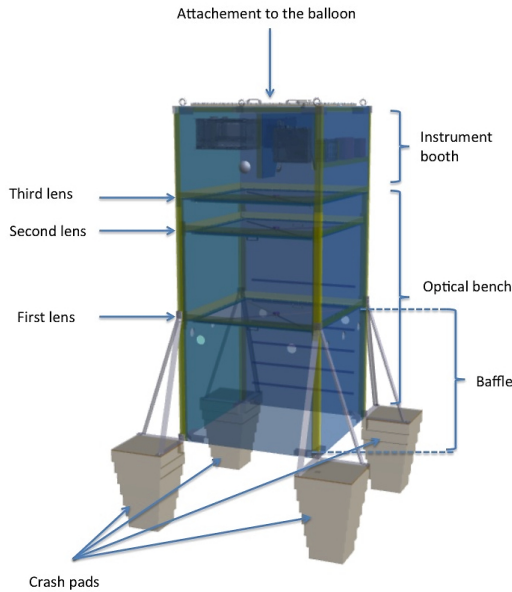


**Figure 1:** EUSO-Balloon Instrument Overview.

mission parameters are justified in section 3 devoted to the subsystems. The parallelepiped-shaped telescope presents a wide field of view of  $12^\circ \times 12^\circ$  for a collecting surface of  $1 \text{ m} \times 1 \text{ m}$ . During observations, it points to nadir observing the earth's atmosphere. The main instrument basically consists of an optical bench associated to a detector module booth placed at the focal position. The optical bench encompasses two Fresnel lenses. The instrument booth includes the whole electronics inside a pressurized watertight box. The instrument booth is delimited by the third lens.

The main instrument includes an external roof-rack, which allows the accommodation of complementary instruments like an infra-red camera developed for atmosphere monitoring [4].

## 2.1 General Characteristics and Functions

The optical subsystem includes the optical bench which focuses parallel light rays onto a finely pixelized focal surface, consisting of an array of Multi-Anode Photomultipliers (MAPMTs) sensitive to UV light in the 290-430 nm range with very good photon-detection efficiency. The Focal Surface (FS) is completed by a complex electronics, which allows fast measurement within microsecond time scale, including photodetector protection against intense light flux by fast switches, auto-triggering capability, event filtering and event recording. The electronics records, for each triggered event, a sequence of 128 consecutive images with a time resolution of one Gate Time Unit (GTU) equal to  $2.5 \mu\text{s}$ .

## 2.2 Instrument Structure

The mechanics of the instrument is made of Fibrelam® panels, arranged together through fiberglass sections. The instrument is coated by an insulating cover to protect the components from fast temperature changes during balloon ascent and descent. Special watertight valves, inserted in the optical bench, are used to enable pressure equilibrium with the external environment. Wherever the after-flight landing location occurs, the instrument must be recovered with the smallest damages. The bottom part is therefore

General parameters	
Field of view	$12^\circ \times 12^\circ$
Aperture	$1 \text{ m} \times 1 \text{ m}$
Optics	
Focal Length	1.62 m
Focal Point Spread (RMS)	2.6 mm
Focal Surface	
Curvature Radius	2.5 m
Number of Pixels	2304
Pixel field of view	$0.25^\circ \times 0.25^\circ$
Pixel size	$2.88 \text{ mm} \times 2.88 \text{ mm}$
BG3 UV Filter transmittance	98 %
Wavelength range	290 nm - 430 nm
Number of MAPMTs	$6 \times 6$
PhotoDetection (MAPMTs)	
Number of channels	64
Photo detection efficiency	$\sim 35 \%$
Gain	$10^6$
Pulse duration	2 ns
Two pulses separation	5 ns
Dynamic Range	$\sim 1 - 1000 \text{ photons}/\mu\text{s}$
Maximum tube current	$100 \mu\text{A}$
Signal Measurement (ASIC)	
Photon Counting (64 ch), photoelectrons	0.3 pe (50 fC) - 30 pe (5 pC)
Charge to Time Conv (8 ch)	2 pC (10 pe) - 200 pC (100 pe)
Shapping time	30 ns
Sampling period (GTU)	$2.5 \mu\text{s}$
Readout Clock	40 MHz
Triggers (FPGA, Virtex 6 (L1) and Virtex 4 (L2))	
L1 rate	7 Hz (1-100 Hz)
L2 rate	Max 50 Hz
Event readout and DAQ (CPU, Clocks, GPS)	
Event size	330 kB
Data flow	3.24 Mb/s
Readout Clock	40 MHz
Event dating	at $\mu\text{s}$ level

**Table 1:** Main features of the EUSO-Balloon instrument

equipped with crash-pads, which absorb strong deceleration (up to 15 g) when landing on ground. A baffle with special holes in the optical bench are used as a piston-effect to damp the shock for a fall over water. The instrument booth, a totally watertight sealed box, consists of a central aluminium plate on which the various electronic boxes are fixed. One of its side is the third lens. The opposite side is an aluminium radiator used to dissipate the heat generated by the electronics. The instrument is surrounded by buoys to avoid sinking in case of splashdown and to raise straight up the instrument booth above the water level.

## 3 The Instrument Subsystems

The main instrument is divided into the following main subsystems: 1) the Optics; 2) The Focal Surface (FS) which includes the photodetector with the MAPMTs, the ASICs measuring signals, the Photo-Detector Module Board (PDMB) and the High Voltage Power Supplies (HVPS); 3) The Data Processing (DP) involving the Cluster Control Board (CCB) providing readout triggers and the Data Acquisition System (DAQ); 4) Utilities like the monitoring also called the housekeeping board (HK) and the low voltages power supplies (LVPS) associated to the batteries (PWP). All these subsystems are all described below.

### 3.1 Optics Subsystem

The optics subsystem includes three lenses. Its goal is to provide the best focusing for the smallest focal distance. The focusing requirement is constrained by the pixel size of the photodetection system. Due to the wide angular field of view, it is necessary to combine 3 flat lenses. The first and third lenses are one-sided focusing Fresnel lenses, while the lens in the middle is purely dispersive, necessary

to correct for chromatic aberrations. They are made of PMMA material [5]. Ray tracing calculations, including the temperature profile expected for flights in cold and warm cases, provide a focal length of 1.62 m and a focal point spread width of  $\sim 2.6$  mm, smaller than the pixel size.

### 3.2 Focal Surface Subsystem

The FS is a slightly curved surface containing one Photo-Detector Module (PDM). The design matches the one of the JEM-EUSO central PDM. A PDM contains 36 MAPMTs and therefore it is an array of  $48 \times 48$  pixels of  $2.88 \text{ mm} \times 2.88 \text{ mm}$  size each, slightly larger than the focal point spread. The PDM is divided into a set of 9 identical Elementary Cells (ECs), which are matrices of  $2 \times 2$  MAPMTs. The photocathode is covered by a BG3 UV filter. Inside the PDM structure, the 9 ECs are disposed and tilted according to the appropriate shape required for the FS. We review in the following the main properties of this electronics.

**MAPMTs** They are Hamamatsu photon detectors (R11265-M64) consisting of a matrix of  $8 \times 8$  pixels. Each pixel is associated to an anode generating a charge or a current in output. Their sensitivity is as low as a few tenths of photon and their dynamic range can extend up to few thousands photons per  $\mu\text{s}$  when working at their nominal high gain of  $10^6$ . The anode signals of the MAPMTs are measured and digitised by the ASICs and managed by an FPGA based PDM board, which performs also the first level trigger selection. More details on the PDM can be found in [6].

**High voltage power supply** MAPMTs are polarised with 14 high voltages. The latter are generated by a high voltage power supply (Cockcroft-Walton, CW type, to limit power consumption). The nominal high voltage of the photocathode is  $-900 \text{ V}$  for a MAPMT nominal gain at  $10^6$ . The effective dynamic range can be extended up to  $10^7$  photons/ $\mu\text{s}$  by reducing gradually the gain from  $10^6$  by successive factors of  $10^2$  down to a gain of 30. Fast switches (SW) responsive at  $\mu\text{s}$  time-scale, adapt the voltage values to tune the MAPMT gain according to the intensity of photon flux. Because a large photon flux generating anode current above  $100 \mu\text{A}$  would destroy the tube, this automatic control system can even switch off the voltage. The switching decision logic is implemented in the FPGA, which reads out the ASICs. In the PDM, there are 9 independent CW with their individual 9 SW, assembled into two separated HVPS boxes, each CW controlling independently the 9 ECs high voltages.

**ASICs** 36 SPACIROC [7] ASICs are used to perform anode signals measurement and digitisation. These ASICs have 64 channels. Their analog inputs are DC-coupled to the MAPMT anodes. They process in parallel the 64 analog signals in two modes: 1) photoelectron counting mode, in a range from 1/3 of photoelectrons up to 100 photoelectrons, by discriminating over a programmable threshold each of the channels; 2) Integrating mode, estimating with a range from 20 pC to 200 pC, a 8 anodes current sum by time over threshold determination. The 64 analog channels are balanced each-other relatively by gain matching over 8-bits. The discrimination voltage level used in the photon-counting is provided by a 10-bit DAC (Digital to Amplitude Converter). In both cases the digitisation is performed by 8-bits counters every GTU. There is no data buffering on the ASIC. The data are transferred, for each GTU, to the FPGA based PDMB at 40MHz.

**PDMB** The instrument includes two trigger stages. The first level trigger (L1) is implemented in the FPGA (Xilinx Virtex 6) of the PDM-Board (PDMB), integrated in the PDM. The PDMB readouts the data from the 36 ASICs into its internal memory (the event buffer) each GTU to compute the L1 trigger. The L1 principle consists in counting an excess of signals over background in groups of  $3 \times 3$  pixels lasting more than a preset persistence time. The background rate is monitored continuously to adjust in real-time the trigger threshold keeping the L1 trigger rate compatible with the DAQ recording rate (a few Hz). The trigger is evaluated each GTU. Because Air-Showers may extend over 100 GTU, this trigger has the buffering capability over 128 consecutive GTU. To reduce the dead-time induced by event readout, the event buffer is doubled.

### 3.3 Data Processing Subsystem

Data acquisition and storage is the task of the Data Processing subsystem (DP). The DP includes the CCB designed to perform the second level trigger L2, described in [8]. For each generated L1 trigger, the CCB reads data corresponding to the 128 consecutive GTU from the PDMB buffer. In JEM-EUSO, the CCB combines information from 9 PDMs, to reduce the trigger rate to about a few Hz or less compatibly with the data storage capabilities of the DAQ. In the case of the EUSO-Balloon, the CCB, based on a Xilinx Virtex-4 FX-60, serves only one PDM and therefore the L2 trigger is not essential. However the L2 functionality will be tested. In addition to perform the second trigger stage, the CCB reads events from PDMB and passes them to the CPU. It also passes clock signals and configuration data to the PDM. The Clock-Board (CLKB), based on a Xilinx Virtex5 FPGA is part of the DP. It generates and distributes the system clock (40 MHz) and the GTU clock (400 kHz, 98% duty cycle) to all devices. A GPS-Board provides information to perform event time tagging data with an accuracy of a few microseconds. The CPU (Motherboard iTX-i2705 model, processor Atom N270 1.6 GHz) merges the event data with the time tagging data to build an event of a size of 330 kB. This implies a data flow of 3MB/s for a 10 Hz L1-L2 trigger. The CPU writes all data on disks (1 TB CZ Octane SATA II 2.5 SSD) and may also send to the balloon telemetry a subset of events flagged by the CCB, to allow monitoring.

**Monitoring** The instrument behaviour is controlled at low frequency by the Housekeeping system (HK) which is a part of the DP. It is based on a commercial micro controller board (Arduino Mega 2560) designed to control temperatures, voltages, and alarms raised by several boards. The CPU polls from time to time the alarms and initiates the corresponding foreseen actions. The HK is connected to the telemetry system to receive basic commands, namely those that allow to turn on-off most of the boards power supplies through relays.

**Power Supply and Electrical Architecture** The instrument runs autonomously thanks to a set of 60 battery cells providing 28 V (225 W during 24 H) to a set of low-voltage boards generating isolated-decoupled lower voltages to the PDM (HVPS and PDMB), DP (CPU,CLKB,GPSB,CCB and HK). The electrical architecture follows the EMC rules to prevent floating reference voltages induced by bad grounding (current ground loop effect).

## 4 Assembly and Tests

After fabrication, the instrument has to be calibrated with great accuracy. The key goal of the calibration is to relate a measured digitised signal into the true number of photons impinging on the focal surface or on the first lens. Thus the optics and the MAPMTs will be calibrated very accurately. Other subsystems like the trigger have to be tested once the instrument is close to final assembly. Each of the subsystems of the instrument are calibrated if necessary and tested before the full integration. We also plan to test the integrated instrument before delivering it to the launch site.

### 4.1 Optical Tests

Even if the focal length of each lens and the combined focal length can be predicted by accurate ray tracing, error budgets are obviously associated to manufacturing. To achieve a resolution smaller than the pixel size, the optimum relative distance between the three lenses and the focal surface will be measured experimentally. This is performed by using a large parallel UV beam along the optical axis, sent over the first lens and measuring the focal length by adjusting the position of a CCD camera to get the narrowest focused spot.

### 4.2 Measuring MAPMT Performances

Each channel of the MAPMT is characterized by its photodetection efficiency and by the gain of the phototubes. Before assembling 4 MAPMTs into an EC, the MAPMTs are sorted according their gain. This allows to assembly ECs with homogeneous MAPMT gain for the same HV [10]. For this, gains have to be initially measured with sensitive, commercial multi-channels charge to digital converters imposing to work with a gain being a factor three above its nominal value (corresponding to HV around -1100 V). Once ECs are assembled, the gain and detection efficiency of each channel are measured with the ASICs at a nominal HV value of -900 V. Both types of measurements are done by illuminating the photocathode with a LED (monitored with a NIST-photodiode). MAPMTs are operated in single photoelectron mode [9] to measure the single photoelectron spectrum for each of the 2304 pixels of the instrument camera. This procedure allows to determine the exact high voltage to be applied to the MAPMTs photocathodes of each EC Units.

### 4.3 ASIC Settings

The ASICs measure the single photoelectron spectra at nominal high voltage for each of the channels by performing a series of runs ramping the discriminator voltage. Since the relative gain of channels inside an EC-Unit can be slightly different, the ASICs allow balancing the discrepancies. This is done once the PDM is mounted and each MAPMT is associated to an ASIC. Then the nominal discriminator threshold, at 1/3 of a photoelectron, to be applied to each ASIC is established.

### 4.4 Trigger Tests

Once the PDM is mounted, including the PDMB, the L1 trigger algorithm performance is checked by illuminating the focal surface by a light spot moving closely to speed-of-light, generated by an "old" persistent-screen scope.

## 4.5 Instrument Tests

Final tests will be performed after integration of all subsystems inside the instrument. A check of the correct final position of lenses and focal surface will be done by lighting up the first lens by a parallel UV beam along the optical axis. The size of the focused point on the focal surface will be minimised by finely adjusting the position of the PDM at the sub-millimetre scale. At the end of the integration and at launch site, basic health tests on the electronics will be performed by directly and uniformly illuminating the focal surface or the first lens by a LED-controlled, in single photon mode, as described in [9].

## 5 Operation and Analysis

During the balloon flight operation, the instrument will be controlled from ground by an operator using a control program [11] interfaced to the TC/TM system (Telecommand and Telemetry) NOSYCA of CNES. At a given altitude reached by the balloon, a command will be issued to turn on the instrument. The HK system will turn on one by one each of the subsystems while monitoring parameters will be downloaded at ground. After the nominal set-up is reached, after having chosen the convenient configuration parameters for the ASICs and the triggers, the balloon operator will launch the DAQ program running on the CPU. Operators will control the basic run parameters, namely the background rate calculated by the PDMB. Conventionally thresholds auto-adapt to the required L1-L2 rates unless the operator forces another mode of trigger settings. At any moment, the instrument can be shut down. This will be certainly done during the descent phase.

## 6 Conclusion

The EUSO-Balloon, a scaled-down pathfinder for the JEM-EUSO mission is being currently built to fly as a payload of a stratospheric balloon launched by CNES. It is by itself a complete autonomous instrument capable to validate the technique at the core of the JEM-EUSO mission. This first flight is expected during the CNES balloon campaign in 2014.

**Acknowledgment:** This work was strongly, technically as well as financially supported by CNES and by the JEM-EUSO collaboration. We thank ESA for supporting the JEM-EUSO team with the activities of the ESA Topical Team on "JEM-EUSO".

## References

- [1] J.H. Adams Jr. *et al.* - JEM-EUSO Collaboration, *Astroparticle Physics* 44 (2013) 76-90
- [2] P. von Ballmoos *et al.*, this proceedings, paper 1171
- [3] T. Mernik *et al.*, this proceedings, paper 875
- [4] M.D. Rodríguez Frías *et al.*, this proceedings, paper 900
- [5] Y. Takazawa *et al.*, this proceedings, paper 1040
- [6] P. Barrillon *et al.*, this proceedings, paper 765
- [7] H. Miyamoto *et al.*, this proceedings, paper 1089
- [8] J. Bayer *et al.*, this proceedings, paper 432
- [9] P. Gorodetzky *et al.*, this proceedings, paper 858
- [10] C. Blaksley, this proceedings, paper 628
- [11] L.W. Piotrowski *et al.*, this proceedings, paper 713